Fizika Nizkikh Temperatur, 2003, v. 29, Nos. 9/10, p. 1135–1139

The vibrational relaxation of CO_2 isolated in solid argon

A. Cenian[1], G. Grigorian[2], and G. Śliwiński[1]

[1]*Institute of Fluid-Flow Machinery, Polish Academy of Sciences, Gdansk 80-952, Poland*
E-mail: cenian@imp.gda.pl

[2]*Institute of Physics, St. Petersburg State University, St. Petersburg 198504, Russia*

For description of the vibrational relaxation of CO_2 molecules embedded in Ar matrix the model based on multiphonon transitions is applied. Rates for the VT and VV processes are determined from a fitting of simulated and experimental data. The calculations confirmed that radiative processes influence significantly the vibrational energy relaxation of CO_2 embedded in solid Ar, e.g., the determined rate for energy transfer between ν_3 and ν_2 mode is significantly lower than that predicted under assumption of the nonradiative relaxation.

PACS: 67.40.Fd

Introduction

A large number of physical and chemical processes in the solid-state involve the vibrational energy relaxation (VER) of molecules. A study of this process for molecules isolated in noble-gas matrices has attracted considerable attention over past years. Among the studied systems a spectacular class constitute the CO, NO, O_3, CO_2 or XeF* in solid Ar [1–4]. The vibrational energy transfer in $^{13}C^{16}O_2$ isolated in solid Ar has been investigated by laser induced fluorescence method [2]. The intense radiation observed in the 16-μm region after strong excitation of the state (00°1) was ascribed to the vibrational stimulated emission. Also, for processes of the type $(11^10(2) \rightarrow \nu_1, 2\nu_2)$ and $(00^01 \rightarrow \nu_1 + \nu_2, 3\nu_2)$ the relaxation times τ_{VT} and τ_{V_3V} were estimated from decay times of stimulated emission basing on the assumption that nonradiative relaxation prevails.

In this work we aim at clarifying the influence of different relaxation channels on populations of vibrational levels using the theory of multiphonon relaxation proposed by Nitzan et al. [5]. Also results of estimation of the VER rate constants for the CO_2/Ar system by comparing the experimental and calculated temporal pulse-shape of radiation are discussed.

In particular, we refer to the experimental results for the $^{13}CO_2$ vibrational-energy relaxation in solid argon under conditions of matrix-to-reagent molecular ratio M/R = 2000 [2]. The laser excitation of the ν_3 ($v = 1$) level of carbon dioxide molecules was found to induce strong emissions $(\nu_1 + \nu_2, 3\nu_2) \rightarrow (\nu_1, 2\nu_2)$ and $(\nu_1, 2\nu_2) \rightarrow \nu_2$ in the spectral region around 16 μm. Their sharp threshold as a function of laser excitation density was interpreted as a signature of vibrational stimulated emission. It is known that the CO_2 molecules are trapped in solid argon in two distinct sites: single substitutional, which is stable, and

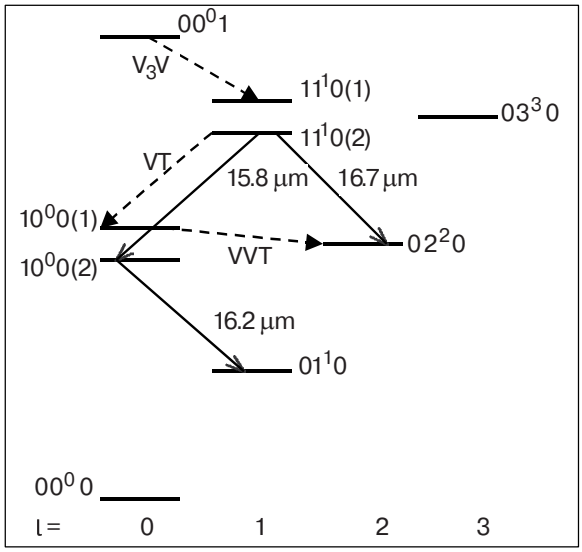

Fig. 1. Diagram of the CO_2 vibrational levels with energy lower than 3000 K; solid arrows denote the transitions of vibrationally stimulated emission observed in Ar matrices, dashed arrows represent the exemplary nonradiative transitions of the type VT, V_3V and VVT.

double substitutional, which appears to be an unstable site [2]. The first one due to the limited free-space is characterized by a stronger vibration-phonon coupling and shorter relaxation times (one order of magnitude). The lasers used in experiments [2], allowed for a good time resolution and a site selective excitation. Both sites were found to be luminescent. The reported emission spectrum due to stable site consisted of three lines (see Fig. 1). The relaxation times τ_{VT} and τ_{V_3V} for processes of the type $(11^10(2) \rightarrow \nu_1, 2\nu_2)$ and $(00^01 \rightarrow \nu_1 + \nu_2, 3\nu_2)$ were estimated in [2] from decay times of the stimulated emission on the assumption that the radiative relaxation may be neglected. In the case of stable site the respective decay times were ~ 700 and ~100 ns.

During final stage of paper preparation, we became aware of the interesting work of Chabbi et al. [6], reporting the rate constants for the VER processes of isolated CO_2, determined by radiation-pulse fitting-procedure using 6 independent constants, i.e., not related by any scaling law.

Model description

The vibrational energy relaxation following strong pulsed excitation is studied by solving the kinetic equations describing the time evolution of populations of different vibrational levels of CO_2 molecules

$$dn_v / dt = R^v_{VT} + R^v_{VVT} + R^v_{V_3V} + R^v_{sp} + R^v_{ind} , \quad (1)$$

where n_v denotes the population of vibrational level v and the R^v terms describe population changes due to the VT, VVT and V_3V intramolecular processes of nonradiative relaxation as well as to spontaneous and induced radiative transitions (the notations are the same as those of Ref. 2). The intermolecular VV processes are neglected because of low concentration of CO_2 in Ar matrix. The Boltzmann-type initial vibrational-distribution is assumed. Excitation is taken into account by a sudden increase of initial vibrational population (N_{001}) of the 00^01 state up to the arbitrary level (fitting parameter).

The equations describing evolution of the photon number has the form:

$$dN_i/dt = R^i_{sp} + R^i_{ind} + R^i_{loss} , \quad (2)$$

where N_i is the number of photons of the ith transition (see Fig. 1), R^i corresponds to photon gain (both through spontaneous and induced processes) and loss processes. The main loss channel is related to the photon leaving the excited region as described in Ref. 2.

For spontaneous emission the Einstein coefficients are applied [7]:

$$A_{v,v-1} = \frac{64\pi^4 \nu^3_{v,v-1}}{3hc^3} \, |\langle v|\mu|v-1\rangle|^2 n \left(\frac{n^2+2}{3}\right)^2 ,$$

where $\nu_{v,v-1}$ is the frequency of the $v \rightarrow v-1$ vibrational transition, $|\langle v|\mu|v-1\rangle|$ is the respective matrix element of the dipole moment and n is the refractive index. The last term describes generally the effects of solid environment.

The stimulated emission cross-section are derived from expression [8]

$$\sigma_{v,v-1} = c^2 A_{v,v-1} / 8\pi\nu^2_{v,v-1} n^2 \gamma ,$$

where γ is the FWHM of the spectral line associated with the $v \rightarrow v-1$ transition of assumed Gaussian profile and estimated to be equal to 0.15 cm^{-1} [2].

For discussion of the nonradiative vibrational-relaxation of a guest molecule in a dense medium several approaches have been proposed [5,9–11]. Here, the relaxation rates are described by the multiphonon relaxation model proposed by Nitzan et al. [5]. This model has proven to provide a satisfactory description of the relaxation for the case of matrix isolated diatomic [12–14]. Accordingly, the rate constant of the $v \rightarrow v-1$ transition is given by [5]

$$K_{v,v-1}(T) = K_{v,v-1}(0) F(T), \quad (3)$$

where $F(T) = (1 + \tilde{n})^N e^{2S\tilde{n}}$ is the temperature coefficient, S is the average vibration-phonon coupling strength (assumed here to be 1), $N = \Delta E_{v,v-1}/h\nu_{ph}$ is the number of matrix phonons involved in dissipation of the vibrational energy gap $\Delta E_{v,v-1}$ in the nonradiative relaxation process, ν_{ph} is the average phonon frequency ($h\nu_{ph}$ = 64 K was assumed for Ar matrix), $\tilde{n} = [\exp(h\nu_{ph}/kT) - 1]^{-1}$ is the phonon occupation number. For low temperatures ($T \sim 5$ K) $\tilde{n} \sim 0$, $F(T) \sim 1$, and $K_{v,v-1}(T) \cong K_{v,v-1}(0)$. The expression

$$K_{v,v-1}(0) = Av \, \frac{e^S S^N}{N!} \, \frac{1}{\Delta E_{v,v-1}} \quad (4)$$

corresponds to the relaxation rate at $T = 0$ K, where A is a constant related to the value of average phonon frequency and the variation of the interaction potential between CO_2 molecules and the surrounding matrix atoms.

Three types of processes are taken into account, and the notation corresponds to that of Ref. 2:

$$\text{VT:} \quad CO_2(\nu_1 + \nu_2, 3\nu_2) + Ar \rightarrow CO_2(\nu_1, 2\nu_2) + Ar, \quad (5)$$

$$\text{VVT:} \quad CO_2(\nu_1, 2\nu_2) + Ar \rightarrow CO_2(\nu_1, 2\nu_2)' + Ar , \quad (6)$$

$$V_3V: \quad CO_2(00^01) + Ar \rightarrow CO_2(\nu_1 + \nu_2, 3\nu_2) + Ar , \quad (7)$$

where $CO_2(\nu_1, 2\nu_2)$ and $CO_2(\nu_1, 2\nu_2)'$ denote different vibrational states of the $(\nu_1, 2\nu_2)$ multiplet at Fermi resonance – see, e.g., [15].

Due to the strong dependence of the rates (3) upon N, only VT processes of $\Delta\nu_2 = 1$ contribute significantly to energy relaxation. The other processes (V_3V and VVT) also proceed with the minimum vibrational energy gap. The VT and V_3V reverse processes responsible for energy transfer from translation to vibration are neglected. However, in the case of VVT processes some rates obtained from the principle of detailed equilibrium are not negligibly small.

Results and discussion

For the stable site emission the time evolution of photon numbers related to radiative profiles is studied in order to get best agreement with experimental data reported in [2]. Accordingly, three fitting parameters A_{VT}, A_{VVT} and A_{V_3V}, related to the constant A in expression (4) for the rates of nonradiative processes, which correspond to transitions of the VT, VVT and V_3V type (Eqs. (5)–(7)) are determined. As a result, all rates for vibrational energy exchange can be calculated. So, this procedure replaces the determination of the seven independent rate constants as proposed in Ref. 6. In both cases, the initial excitation N_{001} is an additional fitting parameter.

The sets of equations (1) and (2) are solved using the GEAR code for numerical integration. Equations describe populations of all the nine vibrational states, which become populated during relaxation process at temperature $T = 5$ K, and photon numbers of the three active radiative-transitions $(\nu_1 + \nu_2, 3\nu_2 \rightarrow \nu_1, 2\nu_2)$ and $(\nu_1, 2\nu_2 \rightarrow \nu_2)$ – see Fig. 1. The terms related to radiation gain and losses were determined from Einstein coefficients, the stimulated emission cross-sections and populations of respective levels. The nonradiative terms were determined by rates (4) scaled by the constants A_{VT}, A_{VVT} and A_{V_3V}.

It should be stressed again that in [2] the following rates for the processes

$$\text{VT:}\quad CO_2(11^10(2)) + Ar \rightarrow CO_2(10^00(1)) + Ar\,,$$
$$K_{VT\_exp} = 1.4\cdot10^6\ s^{-1}\ (\tau_{VT} = 700\ ns), \qquad (5')$$

$$V_3V:\quad CO_2(00^01) + Ar \rightarrow CO_2(11^00(1)) + Ar\,,$$
$$K_{V_3V\_exp} = 10^7\ s^{-1}\ (\tau_{V_3V} = 100\ ns) \qquad (6')$$

were proposed, basing on assumption of nonradiative relaxation. The saturation condition ($N_{001} = 0.5$) for initial excitation was assumed, also.

Results of calculations are presented in Fig. 2–7. Figure 2 demonstrates the evolution of radiation intensity determined by rates scaled (by changing A_{VT} and A_{V_3V}) to the values as proposed in [2] (see dotted line). The assumed value of excitation is evidently too high – as was also confirmed in later considerations on energy conservation [6]. It was found here that the best fit is obtained for $N_{001\_b} = 0.07$, $K_{VT\_b} = K_{VT\_exp}$ and $K_{V_3V\_b} = 0.3K_{V_3V\_exp}$ (see solid line in Fig. 2). A similar value $4\cdot10^6$ s^{-1} for the rate K_{V_3V} was proposed in [6]. The signal profile is not very sensitive to the

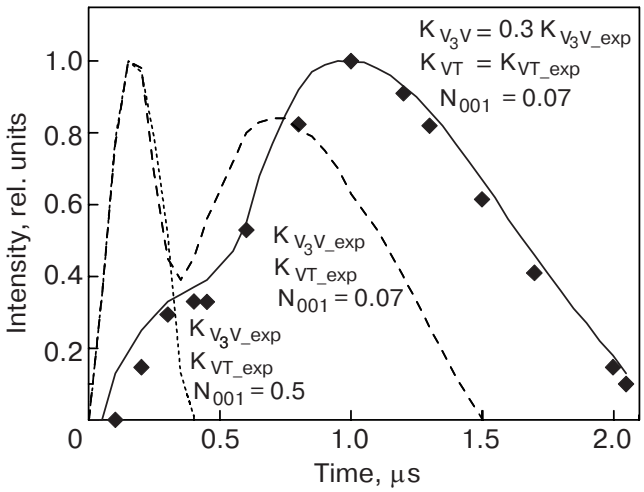

Fig. 2. Time resolved pulse of vibrational stimulated emission from CO_2 located in a stable site of Ar matrix; symbols ♦ correspond to the measurements, lines represent simulations: solid line – for the best fit parameters, dotted line – for the rates determined in [2] and saturation condition ($N_{001} = 0.5$), dashed line – for the rates determined in [2] and $N_{001} = 0.07$.

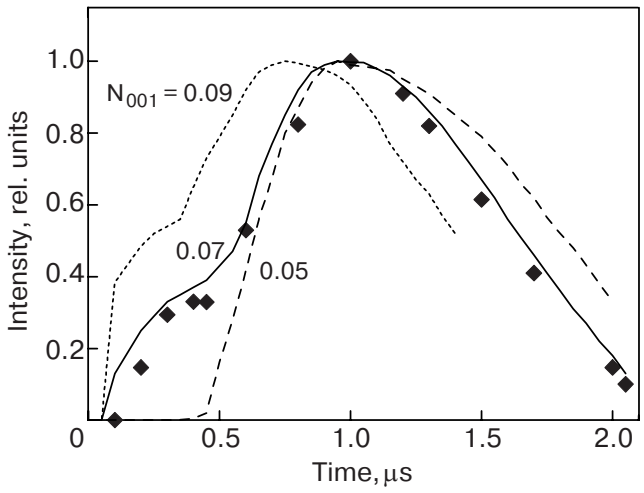

Fig. 3. Time evolution of the stimulated emission pulse from CO_2 located in a stable site of Ar matrix; symbols ♦ correspond to the measurements, lines represent simulations: solid line – for the best fit parameters, dotted line – for optimal rates and $N_{001} = 0.09$, dashed line — for optimal rates and $N_{001} = 0.05$.

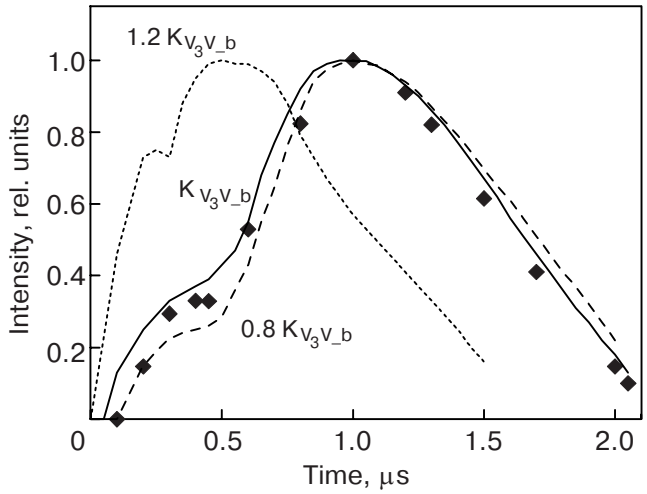

Fig. 4. Same as Fig. 3; solid line — for the best fit parameters, dotted line — for the best fit parameters except $K_{V_3V} = 1.2\ K_{V_3V\_b}$, dashed line – for the best fit parameters except $K_{V_3V} = 0.8\ K_{V_3V\_b}$.

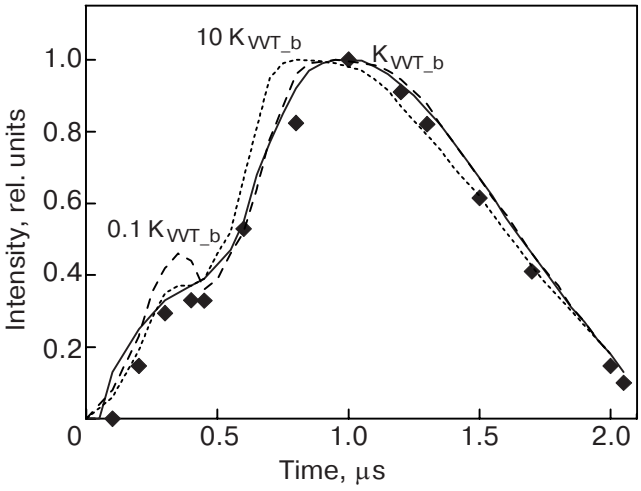

Fig. 6. Same as Fig. 3; solid line — for the best fit parameters, dotted line — for the best fit parameters except $K_{VVT} = 10\ K_{VVT\_b}$, dashed line — for the best fit parameters except $K_{VVT} = 0.1\ K_{VVT\_b}$.

rates of quasiresonant processes of the type (7) as long as they exceed the value of K_{V_3V}. The optimal value of the rate for the process VVT

$$CO_2(10^00(1)) + Ar \rightarrow CO_2(02^20) + Ar\ , \quad (7')$$

$K_{VVT\_b} \sim 10^9\ s^{-1}$ was found and it was assumed for all curves in Fig. 2. Figure 3 presents sensitivity of the profile on the parameter of initial excitation.

The signal profile depends strongly on the rate K_{V_3V} (see Fig. 4). Both the position of maximum and the slope change with the rate variation. The value $K_{V_3V\_b}$ is smaller by a factor of about 1/3 if compared to $K_{V_3V\_exp}$ — this should be related to radiative effects neglected in [2]. It is evident that the radiative processes influence the kinetic seriously, e.g., they determine the temporal scale of the pulse profile. This agrees well with the data reported in [6], and it stays in sharp contrast to the previous assumptions [2]. If we decrease further the rate for the V_3V process, an additional maximum on the temporal pulse-shape appears; clear evidence of the independent radiation from all 3 transitions.

The changes of K_{VT} rate influence the investigated profile much less significantly (see Fig. 5). The rate increase shifts the maximum to smaller value and

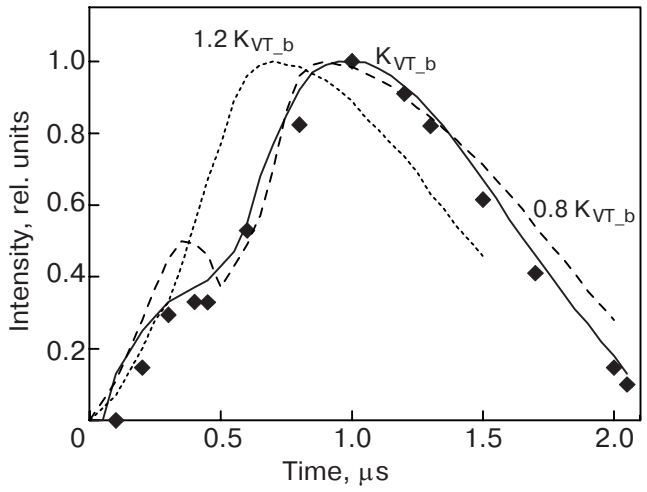

Fig. 5. Same as Fig. 3; solid line — for the best fit parameters, dotted line — for the best fit parameters except $K_{VT} = 1.2\ K_{VT\_b}$, dashed line — for the best fit parameters except $K_{VT} = 0.8\ K_{VT\_b}$.

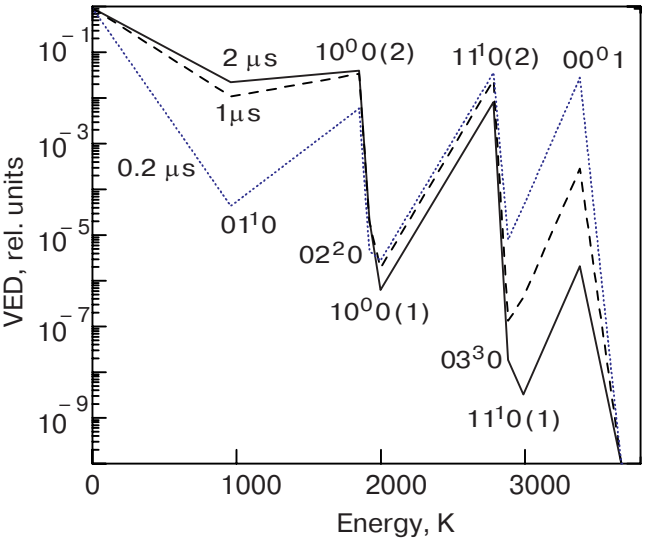

Fig. 7. The Treanor—Likal'ter type of distribution for the best fit parameters and its time evolution; dotted line — 0.2 μs, dashed line — 1 μs, solid line — 2 μs after excitation.

smoothes all structures. In contrast, the K_{VT} decrease leads to more pronounce structures. The profile is even less sensitive to the changes of rates for near resonant transitions (7) — in Fig. 6 we compare the results for K_{VVT} differing two orders of magnitude. Again, the decrease of the K_{VVT} rate leads to structure enforcement, besides it widens also the profile maximum — compare broken and solid lines.

Figure 7 presents the time evolution of vibrational distribution function. The characteristic saw-tooth distribution of Treanor—Likal'ter type, as described previously in detail [15], can be observed. The gradual saturation of the all laser-active transitions ($\nu_1 + \nu_2$, $3\nu_2 \to \nu_1$, $2\nu_2$) and (ν_1, $2\nu_2 \to \nu_2$) is evident.

Conclusion

It was shown that the vibrational relaxation of CO_2 molecules embedded in solid Ar matrix could be well described by the theory of multiphonon transitions. The performed simulations confirmed that radiative processes influence significantly the vibrational energy relaxation of CO_2 embedded in solid Ar, e.g., the determined K_{V_3V} rate is significantly lower than that predicted under assumption of the nonradiative relaxation.

1. D. Jasmin, et al., *J. Chem. Phys*. **108**, 2303 (1998).
2. H. Chabbi, P.R. Dahoo, et al., *Chem. Phys. Lett.* **285**, 252 (1998).
3. G. Zerza, G. Śliwiński, and N. Schwentner, *Appl. Phys*. **A56**, 156 (1993).
4. C. Crepin, M. Broquler, et al., *Laser Chem*. **13**, 65 (1999).
5. A. Nittzan, S. Mukamel, and J. Jontner, *J. Chem. Phys*. **62**, 200 (1975).
6. H. Chabbi, B. Gautier-Roy, et al., *J. Chem. Phys*. **117**, 4436 (2002).
7. E.U. Conder and G.E. Shortley, *Theory of Atomic Spectra*, Cambridge Univ. Press, Cambridge (1967).
8. W. Koecher, *Solid State Laser Engineering*, Springer, Berlin (1996).
9. D.J. Diestler, *J. Chem. Phys.* **60**, 2692 (1974).
10. J. Jortner, *Mol. Phys.* **32**, 379 (1976).
11. S.H. Lin, P.H. Lin, and D. Knittel, *J. Chem. Phys*. **64**, 441 (1976).
12. I.H. Bachir, R. Charneau, and H. Dubost, *Chem. Phys*. **163**, 451 (1992).
13. I.H. Bachir, R. Charneau, and H. Dubost, *Chem. Phys*. **177**, 675 (1993).
14. A. Salloum and H. Dubost, *Chem.Phys*. **189**, 179 (1994).
15. A. Cenian, *Chem. Phys.* **132**, 41 (1989).